Supplement of Biogeosciences, 13, 3343–3357, 2016
http://www.biogeosciences.net/13/3343/2016/
doi:10.5194/bg-13-3343-2016-supplement

Biogeosciences Open Access EGU

Supplement of

The climatic imprint of bimodal distributions in vegetation cover for western Africa

Zun Yin et al.

Correspondence to: Zun Yin (yinzun2000@gmail.com)

1 The Classification And Regression Tree (CART) method and observed bimodality in satellite products

There is a contentious debate about whether the MODIS VCF product [Hansen et al., 2003] is suitable for bimodality research. Hanan et al. [2014, 2015] pointed out that the multimodality found in the MODIS woody cover product [Staver et al., 2011, Hirota et al., 2011] may be attributable to the Classification And Regression Tree (CART) method, which is used for woody cover estimation [Hansen et al., 2003]. Moreover, the aboveground biomass data derived from MODIS NBAR product (MOD43B4.V4, Nadir Bidirectional reflectance distribution function Adjusted Reflections) also used the CART method [Baccini et al., 2008], which might suffer from the same problem. Through data analysis by Baccini et al. [2008] and Staver and Hansen [2015] it shows that the CART method has potential to cause artificial bias in the satellite estimation. However in this supplement we will show that the bimodality in the data sets we used for analysis is not the reflection of the CART algorithm.

1.1 MODIS VCF product (MOD44B)

The key point is whether the observed multimodality is caused by the artificial bias due to CART. To address this question, it is necessary to know where biases and multimodality are located. Figure 1 in Staver and Hansen [2015] provides the validation of the MODIS VCF product. In Fig. 1(b) (validation at Africa), the bias lies between 10–30%. Woody cover at 40% exists in validation data but is absent in MODIS estimation. Simultaneously, bias does not occur at the range between 50 and 70%. Thus if the observed bimodality [Staver et al., 2011, Hirota et al., 2011] was caused by the CART, two peaks in the density distribution will present at 10–30% and 50–70%. However, the threshold of bimodality discovered [Staver et al., 2011, Hirota et al., 2011] is at 60%, implying that the lack of observed woody cover in MODIS at 60% is not caused by the CART.

Further evidence is the histograms of MODIS product and observed data (Figure 2 in Staver and Hansen [2015]). If the bimodality was caused by the CART, there should be a sink of MODIS woody cover at 60% compared with the validation data. However, the histogram of the MODIS product coincides with that of observed data very well (the trend is much clearer for the global region, see Fig. 2(a) in Staver and Hansen [2015]). In this paper we only focus on the bimodality between savanna and forest (gap occurs at 60%). Even if the MODIS product is not well resolved at woody cover values below

30% [Staver and Hansen, 2015], the low woody cover part is still hardly overestimated over 60% by the CART (see Fig. 1 in Staver and Hansen [2015]). Thus we conclude that it is reasonable to consider that part as savanna in our analysis.

1.2 Aboveground biomass data

Figure 5 in Baccini et al. [2008] illustrates the validation of the aboveground biomass data. Note that $1\,\mathrm{Mg\,ha^{-1}}$ is equal to $0.05\,\mathrm{kgC\,m^{-2}}$. Then the threshold found between forest and savanna ($7\,\mathrm{kgC\,m^{-2}}$) is at $140\,\mathrm{Mg\,ha^{-1}}$. Although a bias also exist, it does not effect the bimodality and the threshold. It perfectly meets the requirement raised by Hanan et al. [2015] as: "the discontinuities in satellite estimation should surely be accompanied by similar discontinuities in validation data", when they replied to Staver and Hansen [2015]. Moreover, Baccini et al. [2008] also used another independent source (Lidar GLAS measurements) for validation, which did not use the CART method. Figure 7 in Baccini et al. [2008] illustrates the result. It clearly shows discontinuity in the observed tree height but not in the satellite estimation, implying that the bimodality in the aboveground biomass data set is not effected by the CART , at least at $140\,\mathrm{Mg\,ha^{-1}}$ (equal to $7\,\mathrm{kgC\,m^{-2}}$ in this paper).

2 Bimodality test of the mean annual incoming shortwave radiation $\overline{R}$

The histograms of $\overline{R}$ under different $\overline{P}$ bands are illustrated in Figure S1. In most cases, the distribution shows two peaks and the threshold is approximately around 215–$220\,\mathrm{W\,m^{-2}}$. The ICL of class number is shown in Fig. S2. Although three-class model is shown as the best fit, the ICL value of two classes is very low as well. Moreover, the means of the detected three classes are 184, 200 and $223\,\mathrm{W\,m^{-2}}$. From Fig. S1 we can find that the first two modes are tightly linked and the difference between them is far less than that between the second and the third mode. Thus we decided to select the two-class model and illustrate the fitted normal distributions in Figure. 1e in the manuscript.

3 Special cases of the bimodality test for woody cover W

When the bimodality test is applied on the W in each climatic grid cell, we find that, in some cases, the detected two modes does not mean the coexistence of two land cover types. If the proportion of one detected mode (by the bimodal test) is too low or too high, three types of error will occur, where W is actually unimodal distributed but is detected as bimodality by the test. Thus we set a threshold (5/95%) to avoid the three types of error. If the threshold is reached, we assume the W in the specific grid cell is unimodal distributed.

We collect all climatic grid cells that meet the two conditions: 1) Bimodality of W is detected by the test; 2) The proportion of one detected mode is less/more than 5/95%.

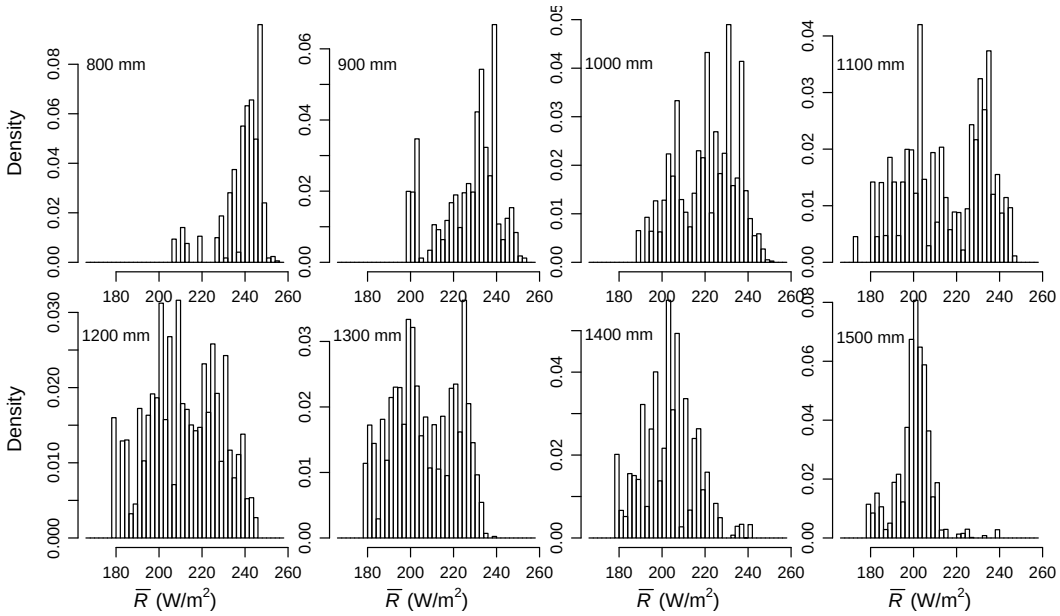

Figure S1: Density distribution of mean annual incoming shortwave radiation $\overline{R}$ under different precipitation bands.

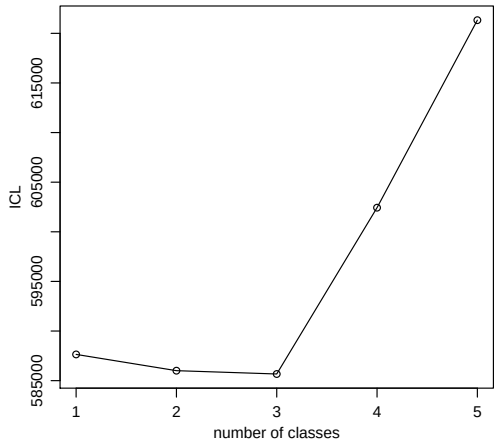

Figure S2: The Integrated Completed Likelihood (ICL) of class numbers of $\overline{R}$ in the whole research region.

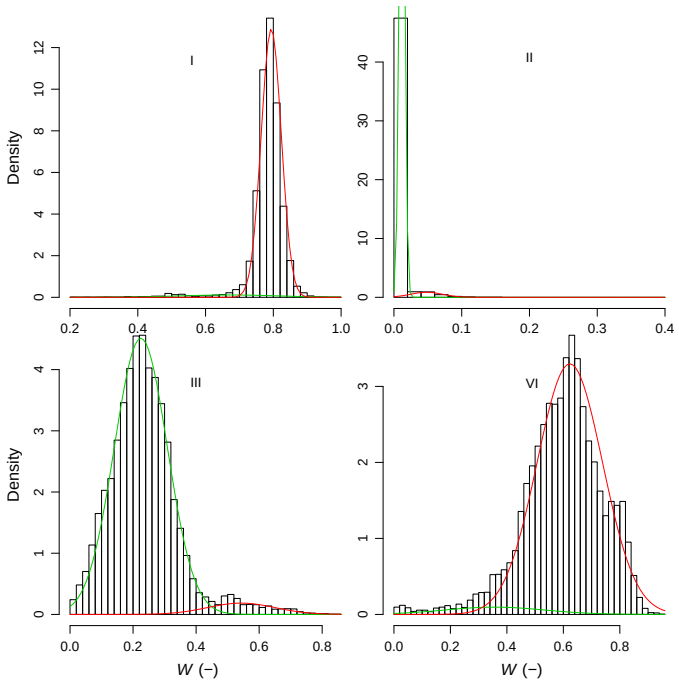

Figure S3: Four special types of W histograms that are detected as bimodal distribution. Red and green lines indicate the two normal distributions that are fitted by the bimodal test.

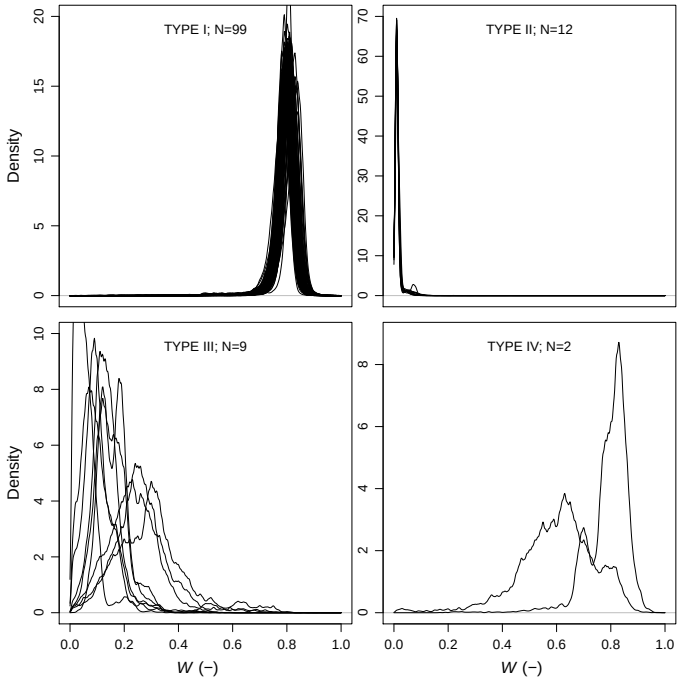

Figure S4: Histograms of W of all grid cells that belong to the four types. N is the number of grid cells in the specific category.

These grid cells can be divided into four categories. Figure S3 shows the W histogram and the fitted normal distributions of one selected grid cell from the specific category. Type I: Bimodality is detected, but the proportion of the savanna state is less than 5%. In this case, the mean of the fitted savanna state (green curve) is over 0.6. Thus we just consider it as unimodal distribution. Type II: Bimodality exists, but both of the modes belong to the treeless case. So we consider it as unimodal. Type III: It is similar to type II, but the two modes belong to the savanna state. Type VI: A special case, but this type only contains two grid cells (Fig. S4). Type I–III are the three types of error discussed above. The type IV is an exception, which only occurs twice. In Figure S4 we illustrate density distributions of all grid cells from the four types. N is the cell number of the specific category.

References

A. Baccini, N. Laporte, S. J. Goetz, M. Sun, and H. Dong. A first map of tropical Africa's above-ground biomass derived from satellite imagery. *Environmental Research Letters*, 3(4):045011, 2008.

Niall P Hanan, Andrew T Tredennick, Lara Prihodko, Gabriela Bucini, and Justin Dohn. Analysis of stable states in global savannas: is the cart pulling the horse? *Global Ecology and Biogeography*, 23(3):259–263, 2014.

Niall P. Hanan, Andrew T. Tredennick, Lara Prihodko, Gabriela Bucini, and Justin Dohn. Analysis of stable states in global savannas –a response to staver and hansen. *Global Ecology and Biogeography*, 24(8):988–989, 2015.

M. C. Hansen, R. S. DeFries, J. R. G. Townshend, M. Carroll, C. Dimiceli, and R. A. Sohlberg. Global percent tree cover at a spatial resolution of 500 meters: First results of the MODIS vegetation continuous fields algorithm. *Earth Interactions*, 7(10):1–15, 2003.

M. Hirota, M. Holmgren, E. H. Van Nes, and M. Scheffer. Global resilience of tropical forest and savanna to critical transitions. *Science*, 334(6053):232–235, 2011.

A. C. Staver, S. Archibald, and S. A. Levin. The global extent and determinants of savanna and forest as alternative biome states. *Science*, 334(6053):230–232, 2011.

A. Carla Staver and Matthew C. Hansen. Analysis of stable states in global savannas: is the cart pulling the horse? –a comment. *Global Ecology and Biogeography*, 24(8): 985–987, 2015.